AIAA JOURNAL
Vol. 58, No. 7, July 2020

Technical Notes

Gas Thermometry by Optical Emission Spectroscopy Enhanced with Probing Nanosecond Plasma Pulse

Xingxing Wang* and Alexey Shashurin†
Purdue University, West Lafayette, Indiana 47907

https://doi.org/10.2514/1.J059511

I. Introduction

IN RECENT years, nanosecond repetitive pulsed (NRP) discharges have been found of great use for combustion-related applications such as increasing flame speed [1,2], enhancing flame stabilization at low fuel/oxidizer ratios [3–6], and mitigating combustion instability [7–10]. In addition, NRP discharges have been applied for aerodynamic flow controls. Surface dielectric barrier discharge plasmas driven by NRP discharges have been explored for controlling boundary layers at realistic flight conditions [11,12], as well as for shock wave modification in supersonic flow [13,14]. NRP spark plasmas have also been shown to be effective at inducing flow instabilities by generating pressure waves [15–17].

Comprehensive temporally resolved measurements of the NRP plasma properties are critical for understanding the nature of the plasmas and practical applications. Two of the most important parameters of theses discharges are the total electron number/electron number density and rotational/vibrational temperatures. Electron number density is a measure of the total electrons produced during discharge, which implies the amount of reactive species produced. In previous works, studies of the total electron numbers of the plasma produced in a high-voltage NRP discharge in a pin-to-pin configuration were conducted at atmospheric pressure and room temperature [18,19], where high-voltage (HV) pulses with peak value of 26 kV and pulsewidth of 100 ns were applied to the pin electrodes at frequency of 1 kHz. The total electron number was measured by Rayleigh microwave scattering technique [20]. It was found that, for the spark discharge, the amount of total electrons produced ranged from 2.4×10^{12} to 1.2×10^{13} and the spatially averaged electron number density ranged from 0.9×10^{14} to 1.0×10^{17} cm^{-3}, respectively, when the gap distance between the pin electrodes was changed from 3 to 9 mm [19].

Rotational temperature is often used as a measure of the bulk gas temperature for the NRP discharges at atmospheric pressure based on fast rotational–translational relaxation and the predominant creation of nitrogen $N_2(C)$ by electron-impact excitation of $N_2(X)$ [21–25]. Vibrational temperatures are typically substantially higher than the rotational, which is indicative of the high-degree nonequilibrium inherent to the NRP discharges. In previous work, both rotational and vibrational temperatures of the NRP plasmas were measured with 5 ns temporal resolution [18]. However, these measurements were limited to only the first approximately 20 ns of the discharge due to the following reason. Rotational and vibrational temperatures were determined from the measurements of the nitrogen second positive system with $\Delta\nu = -2$ based on the classical optical emission spectroscopy (OES) approach to fit that measured spectra with the synthetic one generated numerically. It was observed that the second positive system of nitrogen only existed for the first 20 ns of the discharge event; therefore, rotational and vibrational temperatures were only determined during that initial stage of the discharge. Afterward, the emission of the N_2 second positive system disappeared due to the decrease of the reduced field E/N below the favorable range of about 10^{-16}–10^{-15} $\mathrm{V \cdot cm^2}$ as the dense plasma channel was forming between the discharge electrodes [26].

Therefore, measurements of the gas temperature in atmospheric pressure NRP discharges using the OES technique are limited to only the initial 20 ns after the breakdown (several previous works have evaluated OES measurements on later times but have not proven that these measurements provide actual unperturbed values of the gas temperature [24,25]). However, gas temperature data on a significantly longer timescale than that initial time period (microseconds to milliseconds after the breakdown) are crucial for analysis of flow-induced effects by the NRP actuators and their further applications in combustion systems [27]. This obvious research gap has created the initial motivation for the current work to expand applicability of the simple OES approach beyond the initial 20 ns after the breakdown. This initial motivation had expanded into the broader question of how the standard OES procedure can be used for the temporally resolved gas thermometry in general, even if the gas under testing is not emitting the photons required for the spectra collection.

In this work, we present a novel method of air temperature measurements with 5 ns temporal resolution that can be used for a great variety of applications as a thermometer, e.g., in combustion. The method is based on the classical rotational–vibrational temperature measurements using optical emission spectroscopy of the second positive system of nitrogen in conjunction with probing nanosecond plasma pulse. The probing pulse is used in order to excite the emission of the second positive system at the desired moment of time. We demonstrate that it is physically feasible to establish pulsing probe parameters so that gas heating by the probing pulse itself is negligible, whereas the emission of the second positive system of nitrogen is sufficient to conduct the OES measurements. The spectrum is acquired during the first 5 ns after the probing pulse initiation in order to eliminate the effect of the probing pulse gas heating on the measured temperature. The method is further applied in this work to conduct the gas temperature measurements in the wake of atmospheric NRP discharge from the moment of discharge initiation to 5 ms after the breakdown.

II. Methods and Equipment

The nanosecond plasma pulses were generated between two pin tungsten electrodes. Each tungsten electrode had a tip diameter of approximately 200 μm and was connected to one output arm of an Eagle Harbor nanosecond pulse generator (NSP-3300-20-F) where the gap distance between the electrodes d was kept at 5 mm. A pulse with a peak voltage value of 26 kV and a width of 120 ns was used. The pulse generator was operating in the differential mode such that each output arm of the pulser generated a nanosecond pulse of the same amplitude but opposite polarity with respect to the ground. The voltage was measured by two 30 kV rated high-voltage probes (Tektronix P6015A) connected to each electrode, and the actual voltage applied to the electrodes was calculated as the difference between two probe readings. The current was measured by a current transformer probe (Bergoz FCT-028-0.5-WB) hooked on the positive arm of the pulse generator.

Presented as Paper 2020-0439 at the AIAA SciTech 2020 Forum, Orlando, FL, January 6-10, 2020; received 13 February 2020; revision received 6 April 2020; accepted for publication 27 April 2020; published online 20 May 2020.

*Ph.D. Student, School of Aeronautics and Astronautics.
†Assistant Professor, School of Aeronautics and Astronautics.

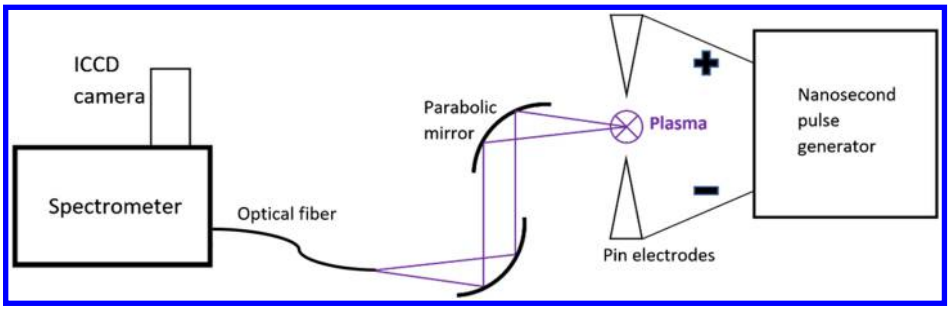

Fig 1. Schematics of the OES measurement system.

An optical emission spectroscopy system was implemented as shown in Fig. 1. A light emission signal was first collected by a parabolic mirror system (with focal length of 4 in.), projected 1:1 onto the input plane of an optic fiber, and then transferred to a spectrometer (Princeton Instrument Acton SpectraPro SP-2750). The converted spectrum data were recorded by an Intensified Charged Coupled Device (ICCD) camera (Princeton Instrument PI-MAX 1024i) mounted onto the spectrometer. A nitrogen second positive system ($C \rightarrow B$) with a spectral band of $\Delta\nu = \nu' - \nu'' = -2$ was captured for further fitting with the synthetic spectra simulated in SPECAIR.

For the temperature measurements in the initial 20 ns of the discharge, the procedure was the same as in previous work [18]. Specifically, the gate width of the ICCD camera was set at 5 ns and a time step at 5 ns. Approximately 50–200 samples were accumulated to achieve an adequate signal-to-noise ratio for further spectrum fitting, depending on the intensity of the emission. For the temperature measurements after the NRP discharge, a second HV probing pulse was applied to the electrodes with the controlled delay in order to initiate additional breakdown and reignite the emission of the second positive system of N_2. The spectrum at the very first 5 ns of the probing pulse was recorded in order to eliminate the effect of gas heating due to the probing pulse on the measured temperature (see details in the following). Five-hundred spectrum samples were accumulated on the ICCD chip to improve the signal-to-noise ratio of the spectrum. The time intervals between the NRP discharge and the probing pulse were chosen to be 20, 50, 100, 200, 500, 1000, 2000, and 5000 μs (20 μs was the earliest time at which we were able to create the probing breakdown with the currently available HV pulse generator). The sample waveform illustrating the NRP discharge pulse and subsequent probing pulse is shown in Fig. 2 with a delay of $\Delta t = 20$ μs. The NRP discharges operated at the repetition frequency of 1 Hz to ensure the temperature relaxation to the room temperature before each next NRP pulse.

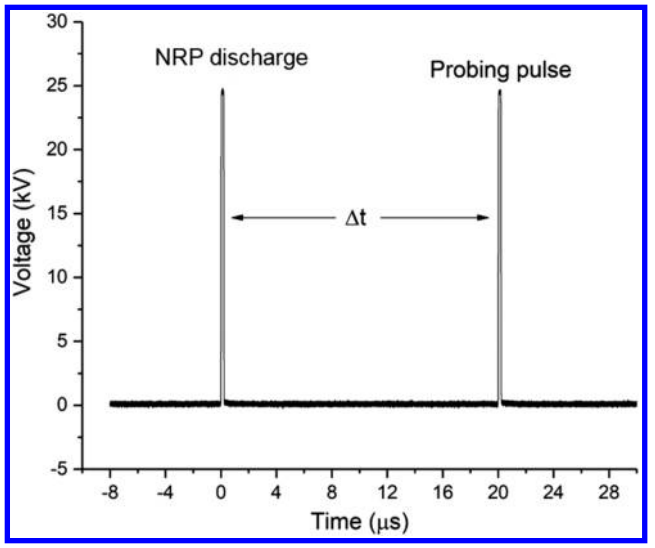

Fig 2. Sample waveform illustrating NRP discharge pulse and subsequent probing pulse applied with delay of $\Delta t = 20$ μs.

III. Results and Discussion

First, the temporal evolution of V, I, T_{rot} and T_{vib} for the initial 20 ns of the NRP discharge has been measured as shown in Fig. 3. One can see the breakdown voltage (approximately 17 kV) was reached at $t = 35$ ns and followed by the discharge current peak of 22 A. Rotational and vibrational temperatures were measured within the time interval of $t = 35$–55 ns with 5 ns temporal resolution using the OES technique. Within this time interval, T_{rot} increases from 300 to 600 K, and T_{vib} increases from 3900 to 5020 K. It was observed that the second positive system of N_2 presented in the emitted spectrum during only the first 20 ns after the breakdown and disappeared thereafter. The examples of the spectra obtained in the first 20 ns after the breakdown ($t = 35$–55 ns) and subsequent 20 ns ($t = 55$–75 ns) are shown in Fig. 4. One can see that multiple spectral bands including the second positive system are clearly detectable only in the spectrum acquired in the first 20 ns. Therefore, T_{rot} and T_{vib} were determined by the OES during the time interval $t = 35$–55 ns only. Vanishing of the N_2 second positive system in the emission spectrum can be explained by the quenching of the corresponding excited vibrational and rotational levels and absence of the new excitations. Indeed, according to Raizer, the reduced electric field $E/N \geq 10^{-15}$ V $\cdot$ cm^{-2} is required for the efficient pumping of the electronic excitations, vibrations, and ionization of O_2 and N_2, whereas efficiency of these transitions decreases for the lower reduced fields [26]. Rough estimations of the reduced electric field based on the discharge voltage experimental data shown in Fig. 3 confirm that the reduced electric field was about 10^{-15} V $\cdot$ cm^{-2} for the initial 20 ns after the breakdown and then dropped significantly due to the creation of a highly conductive spark channel between the electrodes and the associated decrease of the discharge voltage.

Figure 5 shows typical voltage/current waveforms of the probing pulse applied with a delay of $\Delta t = 20$ μs after the NRP discharge. Application of the probing pulse caused additional breakdown of the gas and "reillumination" of the second positive system in the spectrum. The shaded area represents the time window (5 ns) when the spectrum was acquired by the spectrometer. Note that V/I waveforms look very different from that of the NRP pulse shown in Fig. 3 due to the better impedance matching with the pulser caused by the presence of decaying the plasma and heated gas in the gap. As the delay time Δt was increased to several milliseconds, the shape of the V/I waveforms became similar to that shown in Fig. 3 due to the completion of the plasma decay.

The gas temperature evolution after the NRP discharge was determined using this method for probing pulse delays of 20, 50, 100, 200, 500, 1000, 2000, and 5000 μs as shown in Fig. 6. The error bars correspond to the temperature range required to keep the SPECAIR-simulated spectra within the limits of the experimental data spread. Time zero implies the NRP discharge event (same as in Fig. 3). One can see from Fig. 6 that the gas temperature was measured to be approximately 2600 K at 20 μs after the NRP discharge, decreased to around 650 K at 500 μs, and finally reached 300 K at 5 ms after the discharge.

It is critical for the method considered here to confirm that gas heating due to the probing pulse itself is negligible as long as the spectrum of the N_2 second positive system is acquired during the first 5 ns of the probing pulse only. Several previous works have assumed that heating by the probing pulse during the first several nanoseconds

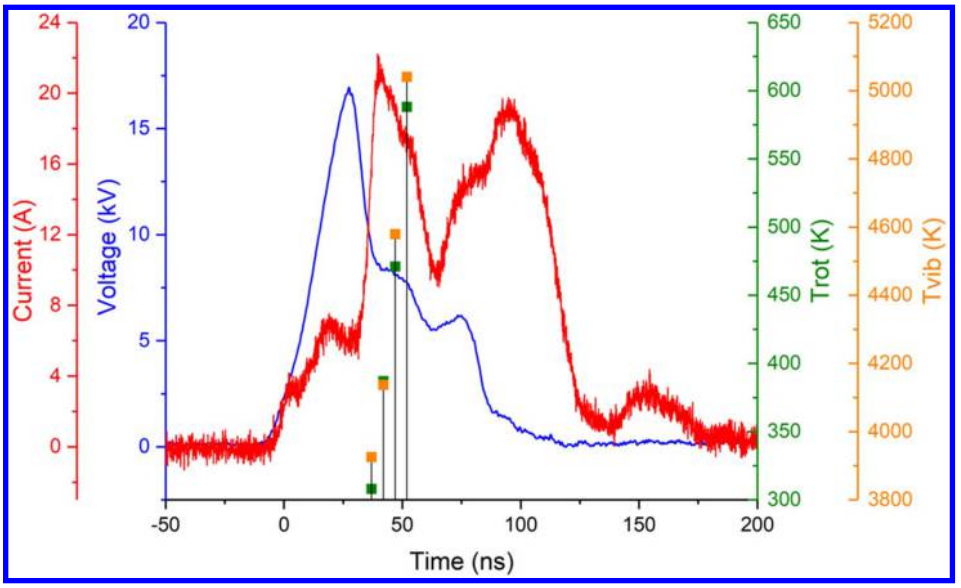

Fig 3. Temporal evolution of V, I, T_{rot}, and T_{vib} for NRP discharge.

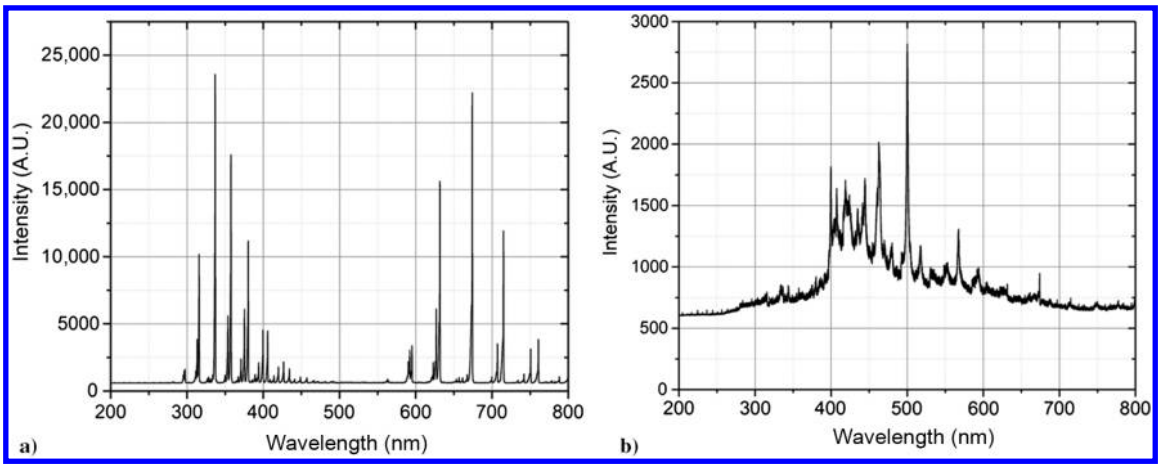

Fig 4. Full spectrum from 200 to 800 nm of the light emission of the discharge: a) initial 20 ns after the breakdown, and b) 20–40 ns after the breakdown (A.U. = arbitrary units).

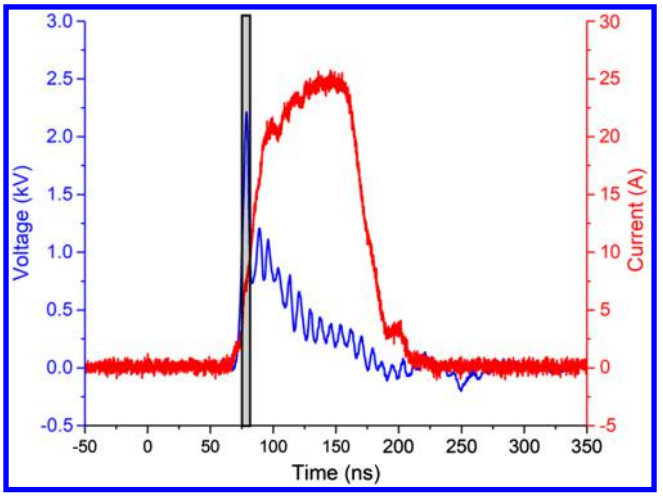

Fig 5. Voltage/current waveform of probing pulse with $\Delta t = 20$ μs. Shaded are represents duration when ICCD camera gate was open. Waveform of probing pulse was different from that of NRP discharge pulse in Fig. 3 due to impedance change between electrodes in wake of NRP discharge.

after its onset is negligible [24,25]. However, this is not a universal fact and requires further proof because the temperature rise is clearly depending on the probing pulse parameters (amplitude; dV/dt); the substantial rise of the rotational temperature can be observed even during the first 5 ns period of the pulse [25]. Therefore, probing pulse parameters should be customized for each specific experiment to make sure that the heating by the probing pulse is negligible, whereas the emission of the second positive system of nitrogen is sufficient to conduct the OES measurements. In this work, the temperatures measured at the first 5 ns of the NRP discharge and at 5 ms after it agree with the true unperturbed room temperature of 300 K. Thus, it can be concluded that gas heating by the specific probing pulse used in this work is negligible on the timescale of 5 ns. Note that the total electrical energy deposition during the first 5 ns of the probing pulse was about four to five times smaller if the probing pulse was applied with a 20 μs delay rather than one applied with a 5 ms delay (see V/I waveforms shown in Figs. 3 and 5): specifically, 0.06 mJ for $\Delta t = 20$ μs and 2.6 mJ for $\Delta t = 5$ ms. And, therefore, the gas heating by the probing pulse applied with a 20 μs delay is expected to be even less pronounced.

The approach proposed here can be used for the temporally resolved gas thermometry in various applications. Specifically, it can be used for combustion thermometry in various gas mixtures

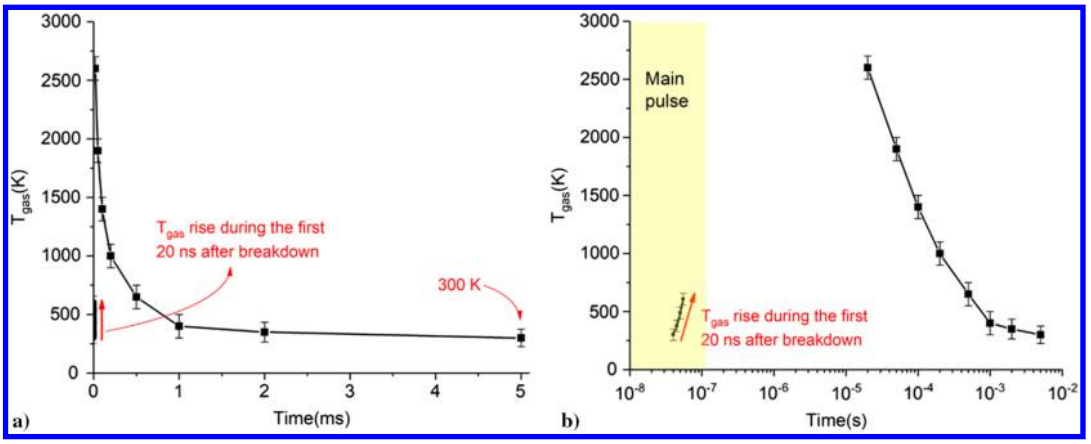

Fig 6. Temporal evolution of rotational temperature measured using the OES technique enhanced by nanosecond probing pulse a) in linear timescale, and b) in log timescale.

and pressure ranges in case Boltzmann distribution of rotational levels in $N_2(C)$ state can be experimentally confirmed. The proposed method is particularly fitted for the temperature measurements in plasma-assisted ignition/combustion systems, which are already equipped with electrodes that can be used for application of the probing pulses. The full spectra of other applications, the impact, and the potential limitations of the current approach are subjects of future works. In comparison with traditional means of temperature measurement, such as the thermocouple, the proposed method is characterized by better temporal resolution (about 5 ns). Spatial resolution of the temperature measurements (down to about 1 mm) can be achieved by appropriate positioning of the electrodes and choosing the gap size. In addition, nonelectrode systems using laser-induced plasma as a probing pulse can be potentially used if insertion of the physical pin electrodes is not possible. The current approach is associated with a similar degree of complexity as spontaneous Raman scattering diagnostics while possessing significantly easier implementation in comparison with the Coherent anti-Stokes Raman Spectroscopy (CARS) technique [28–31].

The proposed method can be further developed as follows. Temperature measurements right after the NRP pulse can be accomplished by choosing higher pulse repetition frequency or by using of a separate HV pulser for creation of the probing pulses along with appropriate synchronization. Measurements of the gas temperature profiles across the spark channel can be conducted by means of imaging the discharge directly onto the slit of the spectrometer. Additionally, this method is to be tested with different gas mixtures at various pressures as a thermometer.

IV. Conclusions

In this work, the novel method of gas temperature measurement using optical emission spectroscopy enhanced with a probing nanosecond plasma pulse is proposed. The method was applied to measure gas temperature evolution up to 5 ms after the NRP discharge. Specifically, for the NRP discharge in a pin-to-pin configuration, the temperature of gas peaked at a value of 2600 K about 20 μs after the discharge and cooled down to about 650 K at 500 μs after the NRP discharge. The proposed method can also be applied for spatially (controlled by the interelectrode gap size) and temporally (down to 5 ns) resolved gas thermometry in various kinds of gas mixtures, e.g., in combustion.

Acknowledgments

This work was supported by the U.S. Department of Energy (grant no. DE-SC0018156) and partially by the National Science Foundation (grant no. 1903415). We thank S. Bane, A. Garner, C. Scalo, and P. Vlachos for useful discussions.

References

[1] Ombrello, T., Won, S. H., Ju, Y., and Williams, S., "Flame Propagation Enhancement by Plasma Excitation of Oxygen. Part I: Effects of O3," *Combustion and Flames*, Vol. 157, No. 10, 2010, pp. 1906–1915. https://doi.org/10.1016/j.combustflame.2010.02.005

[2] Sun, W., Won, S. H., and Ju, Y., "In Situ Plasma Activated Low Temperature Chemistry and the S-Curve Transition in DME/Oxygen/Helium Mixture," *Combustion and Flame*, Vol. 161, No. 8, 2014, pp. 2054–2063. https://doi.org/10.1016/j.combustflame.2014.01.028

[3] Bak, M. S., Kim, W., and Cappelli, M. A., "On the Quenching of Excited Electronic States of Molecular Nitrogen in Nanosecond Pulsed Discharges in Atmospheric Pressure Air," *Applied Physics Letters*, Vol. 98, No. 1, 2011, Paper 011502. https://doi.org/10.1063/1.3535986

[4] Kim, W., Mungal, M. G., and Capelli, M. A., "The Role of In Situ Reforming in Plasma Enhanced Ultra Lean Premixed Methane/Air Flames," *Combustion and Flame*, Vol. 157, No. 2, 2010, pp. 374–383. https://doi.org/10.1016/j.combustflame.2009.06.016

[5] Pham, Q. L., Lacoste, D. A., and Laux, C. O., "Stabilization of a Premixed Methane-Air Flame Using Nanosecond Repetitively Pulsed Discharges," *IEEE Transaction on Plasma Science*, Vol. 39, No. 11, 2011, pp. 2264–2265. https://doi.org/10.1109/TPS.2011.2163806

[6] Pilla, G. L., Lacoste, D. A., Veynante, D., and Laux, C. O., "Stabilization of a Swirled Propane-Air Flame Using a Nanosecond Repetitive Pulsed Plasma," *IEEE Transactions on Plasma Science*, Vol. 36, No. 4, 2008, pp. 940–941. https://doi.org/10.1109/TPS.2008.927343

[7] Lacoste, D. A., Moeck, J. P., Durox, D., Laux, C. O., and Schuller, T., "Effect of Nanosecond Repetitively Pulsed Discharges on the Dynamics of a Swirl-Stabilized Lean Premixed Flame," *Journal of Engineering for Gas Turbines and Power*, Vol. 135, No. 10, 2013, Paper 101501. https://doi.org/10.1115/1.4024961

[8] Lacoste, D. A., Xu, D. A., Moeck, J. P., and Laux, C. O., "Dynamic Response of a Weakly Turbulent Lean-Premixed Flame to Nanosecond Repetitively Pulsed Discharges," *Proceedings of the Combustion Institute*, Vol. 34, No. 2, 2013, pp. 3259–3266. https://doi.org/10.1016/j.proci.2012.07.017

[9] Moeck, J. P., Lacoste, D. A., Durox, D., Guiberti, T. F., Schuller, T., and Laux, C. O., "Stabilization of a Methane-Air Swirl Flame by Rotating Nanosecond Spark Discharges," *IEEE Transactions on Plasma Science*, Vol. 42, No. 10, 2014, pp. 2412–2413. https://doi.org/10.1109/TPS.2014.2323130

[10] Moeck, J. P., Lacoste, D. A., Laux, C. O., and Paschereit, C. O., "Control of Combustion Dynamics in a Swirl-Stabilized Combustor with Nanosecond Repetitively Pulsed Discharges," *51th AIAA Aerospace Sciences Meeting*, AIAA Paper 2013-0565, 2013. https://doi.org/10.2514/6.2013-565

[11] Roupassov, D. V., Nikipelov, A. A., Nudnova, M. M., and Starikovskii, A. Y., "Flow Separation Control by Plasma Actuator with Nanosecond Pulsed-Periodic Discharge," *AIAA Journal*, Vol. 47, No. 1, 2009, pp. 168–185. https://doi.org/10.2514/1.38113

[12] Little, J., Takashima, K., Nishihara, M., Adamovich, I., and Samimy, M., "Separation Control with Nanosecond-Pulse-Driven Dielectric Barrier Discharge Plasma Actuators," *AIAA Journal*, Vol. 50, No. 2,

2012, pp. 350–365.
https://doi.org/10.2514/1.J051114

[13] Nishihara, M., Takashima, K., Rich, J. W., and Adamovich, I. V., "Mach 5 Bow Shock Control by a Nanosecond Pulse Surface Dielectric Barrier Discharge," *Physics of Fluids*, Vol. 23, No. 6, 2011, Paper 066101.
https://doi.org/10.1063/1.3599697

[14] Kinefuchi, K., Starikovskiy, A. Y., and Mile, R. B., "Control of Shock Wave–Boundary Layer Interaction Using Nanosecond Dielectric Barrier Discharge Plasma Actuators," *52nd AIAA/SAE/ASEE Joint Propulsion Conference*, AIAA Paper 2016-5070, 2016.
https://doi.org/10.2514/6.2016-5070

[15] DeBlauw, B., Elliot, G., and Dutton, C., "Active Control of Supersonic Base Flows with Electric Arc Plasma Actuators," *AIAA Journal*, Vol. 52, No. 7, 2014, pp. 1502–1517.
https://doi.org/10.2514/1.J052585

[16] Samimy, M., Kearney-Fischer, M., Kim, J. H., and Sinha, A., "High-Speed and High-Reynolds-Number Jet Control Using Arc Filament Plasma Actuators," *Journal of Propulsion and Power*, Vol. 28, No. 2, 2012, pp. 269–280.
https://doi.org/10.2514/1.B34272

[17] Utkin, Y. G., Keshav, S., Kim, J. H., Kastner, J., Adamovich, I. V., and Samimy, M., "Development and Use of Localized Arc Filament Plasma Actuators for High-Speed Flow Control," *Journal of Physics D: Applied Physics*, Vol. 40, No. 3, 2007, pp. 685–694.
https://doi.org/10.1088/0022-3727/40/3/S06

[18] Wang, X., Jagannath, R., Bane, S., and Shashurin, A., "Experimental Study of Modes of Operation of Nanosecond Repetitive Pulsed Discharges in Air," *AIAA SciTech*, AIAA Paper 2019-1005, 2019.
https://doi.org/10.2514/6.2019-1005

[19] Wang, X., Stockett, P., Jagannath, R., Bane, S., and Shashurin, A., "Time-Resolved Measurements of Electron Density in Nanosecond Pulsed Plasmas Using Microwave Scattering," *Plasma Source Science Technology*, Vol. 27, July 2018, Paper 07LT02.
https://doi.org/10.1088/1361-6595/aacc06

[20] Shashurin, A., Shneider, M. N., Dogariu, A., Miles, R. B., and Keidar, M., "Temporary-Resolved Measurement of Electron Density in Small Atmospheric Plasmas," *Applied Physics Letters*, Vol. 96, No. 17, 2010, Paper 171502.
https://doi.org/10.1063/1.3389496

[21] Starikovskiy, A., and Aleksandrov, N., "Plasma-Assisted Ignition and Combustion," *Progress in Energy and Combustion Science*, Vol. 39, No. 1, 2013, pp. 61–110.
https://doi.org/10.1016/j.pecs.2012.05.003

[22] Wang, Q., Doll, F., Monnedlly, V. M., Economou, D. J., Sadeghi, N., and Franz, G. F., "Experimental and Theoretical Study of the Effect of Gas Flow on Gas Temperature in an Atmospheric Pressure Microplasma," *Journal of Physics D: Applied Physics*, Vol. 40, No. 14, 2007, pp. 4202–4211.
https://doi.org/10.1088/0022-3727/40/14/015

[23] Bruggeman, P. J., Sadeghi, N., Schram, D. C., and Linss, V., "Gas Temperature Determination from Rotational Lines in Non-Equilibrium Plasmas: A Review," *Plasma Source Science Technology*, Vol. 23, No. 2, 2014, Paper 023001.
https://doi.org/10.1088/0963-0252/23/2/023001

[24] Adams, S., Miles, J., Ombrello, T., Brayfield, R., and Lefkowitz, J., "The Effect of Inter-Pulse Coupling on Gas Temperature in Nanosecond-Pulsed High-Frequency Discharges," *Journal of Physics D: Applied Physics*, Vol. 52, No. 35, 2019, Paper 355203.
https://doi.org/10.1088/1361-6463/ab27ef

[25] Rusterholz, D. L., Lacoste, D. A., Stancu, G. D., Pai, D. Z., and Laux, C. O., "Ultrafast Heating and Oxygen Dissociation in Atmospheric Pressure Air by Nanosecond Repetitively Pulsed Discharges," *Journal of Physics D: Applied Physics*, Vol. 46, No. 46, 2013, Paper 464010.
https://doi.org/10.1088/0022-3727/46/46/464010

[26] Raizer, Y. P., *Gas Discharge Physics*, Springer–Verlag, Berlin, 1991, pp. 350–352.

[27] Singh, B., Rajendran, L. K., Giarra, M., Vlachos, P. P., and Bane, S. P. M., "Measurement of the Flow Field Induced by a Spark Plasma Using Particle Image Velocimetry," *Experiments of Fluids*, Vol. 59, No. 179, 2018, pp. 1–15.
https://doi.org/10.1007/s00348-018-2632-y

[28] Lo, A., Cessou, A., Boubert, P., and Vervisch, P., "Space and Time Analysis of the Nanosecond Scale Discharge in Atmospheric Pressure Air: I. Gas Temperature and Vibrational Distribution Function of N_2 and O_2," *Journal of Physics D: Applied Physics*, Vol. 47, No. 11, 2014.
https://doi.org/10.1088/0022-3727/47/11/115201

[29] Dennis, C. N., Slabaugh, C. D., Boxx, I. G., Meier, W., and Lucht, R. P., "5 kHz Thermometry in a Swirl-Stabilized Gas Turbine Model Combustor Using Chirped Probe Pulse Femtosecond CARS. Part 1: Temporally Resolved Swirl-Flame Thermometry," *Combustion and Flame*, Vol. 173, June 2016, pp. 441–453.
https://doi.org/10.1016/j.combustflame.2016.02.033

[30] Roy, S., Kulatilaka, W. D., Richardson, D. R., Lucht, R. P., and Gord, J. R., "Gas-Phase Single-Shot Thermometry at 1 kHz Using fs-CARS Spectroscopy," *Optics Letters*, Vol. 34, No. 24, 2009, Paper 3857.
https://doi.org/10.1364/OL.34.003857

[31] Lo, A., Cleon, G., Vervisch, P., and Cessou, A., "Spontaneous Raman Scattering: A Useful Tool for Investigating the Afterflow of Nanosecond Scale Discharges in Air," *Applied Physics B*, Vol. 107, No. 1, 2012, pp. 229–242.
https://doi.org/10.1007/s00340-012-4874-3

Y. Ju
Associate Editor